

■ Polymers | Very Important Paper |

VIP Insights into the Asymmetric Heterogeneous Catalysis in Porous Organic Polymers: Constructing A TADDOL-Embedded Chiral Catalyst for Studying the Structure–Activity Relationship^[**]

Wan-Kai An,^[a] Man-Yi Han,^[a] Chang-An Wang,^[a] Si-Min Yu,^[a] Yuan Zhang,^[a] Shi Bai,^[a] and Wei Wang^{*[a, b]}

Abstract: Construction of porous organic polymers (POPs) as asymmetric catalysts remains as an important but challenging task. Herein, we exploit the “bottom-up” strategy to facilely synthesize an $\alpha,\alpha,\alpha',\alpha'$ -tetraaryl-1,3-dioxolane-4,5-dimethanol (TADDOL)-based chiral porous polymer (**TADDOL-CPP**) for highly efficient asymmetric catalysis. Constructed through the covalent linkages among the three-dimensional rigid monomers, **TADDOL-CPP** possesses hierarchical porous structure, high Brunauer–Emmett–Teller (BET) surface area, together with abundant and uniformly-distributed chiral sites. In the presence of $[\text{Ti}(\text{O}i\text{Pr})_4]$, **TADDOL-CPP** acts as a highly efficient and recyclable catalyst in the asymmetric addition of diethylzinc (Et_2Zn) to aromatic aldehydes. Based

on the direct observation of the key intermediates, the reaction mechanism has been revealed by solid-state ^{13}C magic-angle spinning (MAS) NMR spectroscopy. In combination with the catalytic testing results, characterization on the working catalyst provides further information for understanding the structure–activity relationship. We suggest that the catalytic activity of **TADDOL-CPP** is largely affected by the structural rigidity, cooperative catalysis, local chiral environment, and hierarchical porous framework. We expect that the information obtained herein will benefit to the designed synthesis of robust POP catalysts toward practical applications.

Introduction

Rooted in the structure–property–activity relationship, the application-oriented strategy has been serving as a rational approach for the designed synthesis of functional materials.^[1–11] For example, porous organic polymers (POPs)^[1–7,9–11] have recently emerged as new and promising materials for potential applications in gas storage/separation,^[3–6,9–13] light-harvesting,^[14] and molecular recognition/sensors,^[15] mainly due to their porous structure and π -conjugation network. Particularly, in view of the high porosity, enhanced stability, and tunable property, the POP materials embedded with catalytic moieties could possibly work as new candidates for heterogeneous catalysts.^[9,10,16–23] For example, POP materials were first applied as

the metal supports for heterogeneous catalysis.^[17a–f] In 2010, the first metal-free POP catalyst^[18] was constructed by the “bottom-up” approach,^[24] through which the Tröger’s base was directly embedded as the catalytic moiety into the material network. This functional POP material was applied as an achiral heterogeneous catalyst that showed comparable activity as the homogeneous Tröger’s base. This application-oriented “bottom-up” strategy has therefore opened up a new approach to connecting nanoporous organic polymers with heterogeneous catalysis. In comparison with the traditional “anchored” heterogeneous catalysts,^[25] the POP catalysts prepared by this way possess easily accessible, highly concentrated, and homogeneously distributed catalytic sites.^[26] However, the structure–property–activity relationship is largely unknown for the POP catalysts because of the limited examples available so far. In this work, we exploit the “bottom-up” strategy to construct a TADDOL-functionalized chiral POP material (denoted as **TADDOL-CPP**, Scheme 1) for highly efficient asymmetric catalysis. We focus herein on the understanding of the catalytic mechanism for the POP materials, especially of the relationship between the chiral porous structure and the enantioselective control of the **TADDOL-CPP** catalyst.

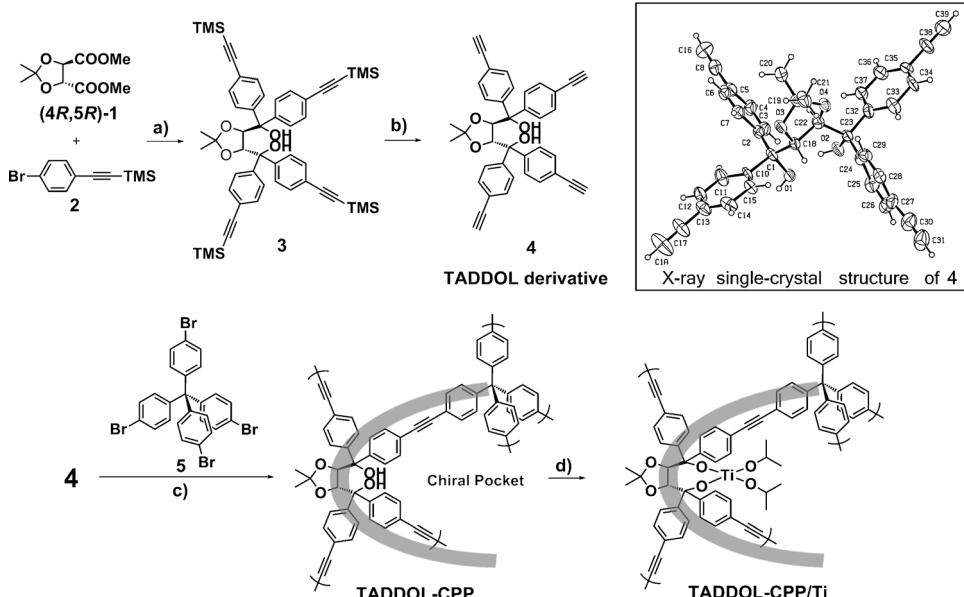
Over the past 30 years, asymmetric catalysis has appeared as one of the most significant frontiers in organic synthetic research.^[27] Remarkable progress has been made in the development of efficient chiral catalysts for numerous enantioselective reactions.^[27,28] However, only a handful of homogeneous asym-

[a] W.-K. An, Dr. M.-Y. Han, Dr. C.-A. Wang, Dr. S.-M. Yu, Dr. Y. Zhang,
Prof. Dr. S. Bai, Prof. Dr. W. Wang
State Key Laboratory of Applied Organic Chemistry
College of Chemistry and Chemical Engineering
Lanzhou University, Lanzhou
Gansu 730000 (P.R. China)

[b] Prof. Dr. W. Wang
Collaborative Innovation Center of
Chemical Science and Engineering
Tianjin 300071 (P.R. China)
E-mail: wang_wei@lzu.edu.cn

[**] TADDOL = tetraaryl-1,3-dioxolane-4,5-dimethanol.

Supporting information for this article is available on the WWW under
<http://dx.doi.org/10.1002/chem.201403002>.



Scheme 1. “Bottom-up” construction of TADDOL-embedded chiral porous polymer (**TADDOL-CPP**) through a concise three-step route. As shown in the X-ray single-crystal structure of the functional building block **4**, the four benzene rings are positioned as butterfly wings, which could offer the steric shielding for asymmetric catalysis. To investigate the cooperative nature of the working catalyst for the asymmetric addition reaction of Et_2Zn to aromatic aldehydes, the **TADDOL-CPP** was further treated with $[\text{Ti}(\text{O}i\text{Pr})_4]$ to afford the **TADDOL-CPP/Ti** (see the main text for details). Reagents and conditions: a) $\text{Mg}, \text{I}_2, \text{THF}$, under Ar, 80°C , 7 h; b) $\text{K}_2\text{CO}_3, \text{CH}_3\text{OH}$, RT, 2 h; c) $[\text{Pd}(\text{PPh}_3)_2\text{Cl}_2], \text{CuI}, \text{PPh}_3, \text{DMF}, \text{Et}_3\text{N}$, under Ar, 80°C , 3 d; d) $[\text{Ti}(\text{O}i\text{Pr})_4]$, toluene, under Ar, RT, 16 h.

metric reactions have successfully been transferred into industrial applications.^[28] One of the main challenges is that most of the scaling-up processes suffer from the costly preparation of the chiral catalysts/ligands and from the tedious separation of the reaction products.^[26] An effective solution to these vital problems is therefore to prepare the heterogeneous chiral catalysts that can be easily recycled and reused.^[26, 29] In this context, the chiral and porous POP catalysts, if they can be constructed, meet these requirements and possess additional advantages by providing accessible catalytic sites and facilitating the mass transport.

Very few chiral POPs have been reported to date.^[20–23] Towards the potential applications of chiral POP catalysts, further development is expected to meet the following criteria: 1) The synthesis of chiral POP catalysts should be concise and based on inexpensive and readily available chemicals; 2) The porous frameworks are robust and embedded with highly accessible catalytic sites; 3) The catalysts should possess excellent catalytic performance in the stereoselectivity together with the reaction yield; 4) The catalysts are reusable and easily recyclable. In addition, it would be highly desirable that the catalytic properties of the POP catalysts can be tuned upon the understanding of the structure–property–activity relationship.

According to these criteria, we report herein the designed synthesis, characterization, asymmetric catalysis, and mechanistic study of a TADDOL-based chiral porous polymer, **TADDOL-CPP**. As shown in Scheme 1, “bottom-up” incorporation of chiral TADDOL moieties into the POP network was facilely achieved in three steps from the simple reagents. Moreover, the resulting **TADDOL-CPP** material is an excellent heterogeneous

porous catalyst for the asymmetric addition reaction of Et_2Zn to aromatic aldehydes. In the presence of $[\text{Ti}(\text{O}i\text{Pr})_4]$, **TADDOL-CPP** presents excellent enantioselectivity control (up to 94% enantiomeric excess (ee)) to a variety of aldehyde substrates and could be easily recovered and reused for at least 11 iterative cycles.

Along with the catalytic testing results, the detailed characterization on the working **TADDOL-CPP/Ti** catalyst provided insightful information on the structure–property–activity relationship. Specifically, the transformation of ^{13}C -labeled benzaldehyde reactant on the catalyst was directly monitored by solid-state ^{13}C NMR spectroscopy. We propose that the excellent catalytic activity of chiral **TADDOL-CPP** is attributed to the rigid network, evenly dispersed dihydroxy sites, local “chiral pocket”,^[31] and hierarchical^[32] porous structure. The information disclosed herein should therefore shed light on the designed synthesis of robust POP catalysts towards the industrial applications.

Results and Discussion

Designed synthesis and characterization of TADDOL-CPP

Derived from tartaric acid, TADDOLs and their derivatives have been playing a key role in the asymmetric synthesis, racemic mixture separation, supramolecular chemistry, and the preparation of chiral liquid crystals and NMR-shift reagents.^[32] In particular, beneficial from the strong interactions such as those between the dihydroxy groups and various H-bond receptors,^[33, 34] TADDOLs and their derivatives could act as efficient catalysts or ligands to catalyze a variety of highly enantioselective reactions.^[35–44] Because of the catalytic importance of the TADDOL family, heterogenization onto various supports^[34, 45–50] through the post-synthesis^[34, 45–48] or copolymerization strategy^[34, 45, 50] has been attempted. For example, targeting the recyclable use of the TADDOL catalysts, Seebach and co-workers have reported the successful immobilization of TADDOLs on resin,^[34] silica gel,^[47] and dendrimers.^[34, 49] It should be noted that the post-synthetic immobilization in general suffers from the disadvantages^[25] of tedious synthetic efforts, less and uneven catalytic sites, and poor stability of the catalyst.

Compared with the immobilization strategy, the “bottom-up” approach applied herein (Scheme 1) not only enables a convenient construction of **TADDOL-CPP** porous network,

but also guarantees the uniform distribution of catalytic TADDOL sites. Moreover, to improve the BET surface area and the pore volume of the POP material, three-dimensional rigid monomers **4** and **5** were selected in our design as the functional and structural building blocks, respectively. Starting from the commercially available tartaric acid derivative (*4R*, *5R*)-**1**, the synthesis of tetraethyl TADDOL derivative **4** could be easily performed by using the Grignard reaction^[38b,51] followed by the deprotection of the trimethylsilyl (TMS) groups (Scheme 1). The **TADDOL-CPP** catalyst was, therefore, easily prepared with a yield of 97% through the Sonogashira–Hagi-hara cross-coupling reaction of **4** and the structural monomer, tetrakis(4-bromophenyl)methane **5**, at 80 °C (see the Experimental Section for details). The thermogravimetric analysis (TGA) revealed that **TADDOL-CPP** was stable up to 270 °C under a nitrogen atmosphere (the Supporting Information, Figure S1). The powder X-ray diffraction (XRD) spectrum of **TADDOL-CPP** displayed broad peaks (the Supporting Information, Figure S2). Meanwhile, the scanning electron microscopy (SEM) and transmission electron microscope (TEM) showed that **TADDOL-CPP** consisted of platelet-like units (30–50 nm in size) with rough surfaces (the Supporting Information, Figures S4 and S5).

The covalent bonding in **TADDOL-CPP** was confirmed by solid-state ¹³C cross-polarization magic-angle spinning (CP/MAS) NMR spectroscopy (Figure 1). As shown in Figure 1b, the ¹³C NMR spectroscopic signals at $\delta=122$, 128, 130, and 145 ppm can be assigned to the carbon atoms on the phenyl rings. The peak at $\delta=26$ ppm corresponds to the methyl

group, whereas those at $\delta=78$ and 108 ppm are assigned to the carbon atoms on the 1,3-dioxolane ring. Meanwhile, the signals at $\delta=64$ and 67 ppm are characteristic for the quaternary carbon atoms on the tetrakis(phenyl)methane moieties.^[12,22,52] **TADDOL-CPP** network also showed the ¹³C NMR spectroscopic signal of the internal alkyne group ($C_{Ar}-C\equiv C-C_{Ar}$) at $\delta=89$ ppm.^[1,18,19] For the purpose of comparison, the liquid ¹³C NMR spectrum of the monomer **4** is also shown (Figure 1a). It can be seen that the chemical shifts of the ¹³C NMR spectroscopic signals for **TADDOL-CPP** (Figure 1b) are in agreement with those observed for **4** (Figure 1a) in a liquid. In addition, the FTIR spectrum of **TADDOL-CPP** (the Supporting Information, Figure S3) showed a strong vibration peak at 3430 cm⁻¹ (characteristic for the dihydroxyl groups in the TADDOL moiety), together with a weak peak at 2200 cm⁻¹ (corresponding to the $-C\equiv C-$ stretching). All these data provided overwhelming evidence for the successful incorporation of TADDOL moieties into the **TADDOL-CPP** network. Furthermore, as calculated from the integration of the peak area at $\delta=26$ ppm in the quantitative ¹³C high-power proton decoupling (HPDEC) MAS NMR spectra (the Supporting Information, Figure S9), the TADDOL content in **TADDOL-CPP** was determined as 0.93 mmol g⁻¹ (see the Supporting Information for the calculation details). This value (theoretical value of 1.14 mmol g⁻¹) is much higher than those reported^[34,45–48] for TADDOL-immobilized catalysts. For example, in the controlled-pore glass (CPG)-bound materials,^[47] the highest TADDOL content is only 0.32 mmol g⁻¹.

The nitrogen sorption measurements at 77 K verified the co-existence of micropores (55% of total surface area) and mesopores (45% of total surface area) in **TADDOL-CPP** (the Supporting Information, Figure S7). Thus, constructed from the rigid three-dimensional building blocks **4** and **5**, **TADDOL-CPP** exhibits the expected high Brunauer–Emmet–Teller (BET) surface area (781 m² g⁻¹) and pore volume (0.43 cm³ g⁻¹). Moreover, the hierarchical porous structure may have a unique advantage: The micropores offer the confined space for a better stereocontrol, whereas the mesopores facilitate the mass transport of the reactants and products during the catalytic process.^[32] This issue will be discussed in detail later.

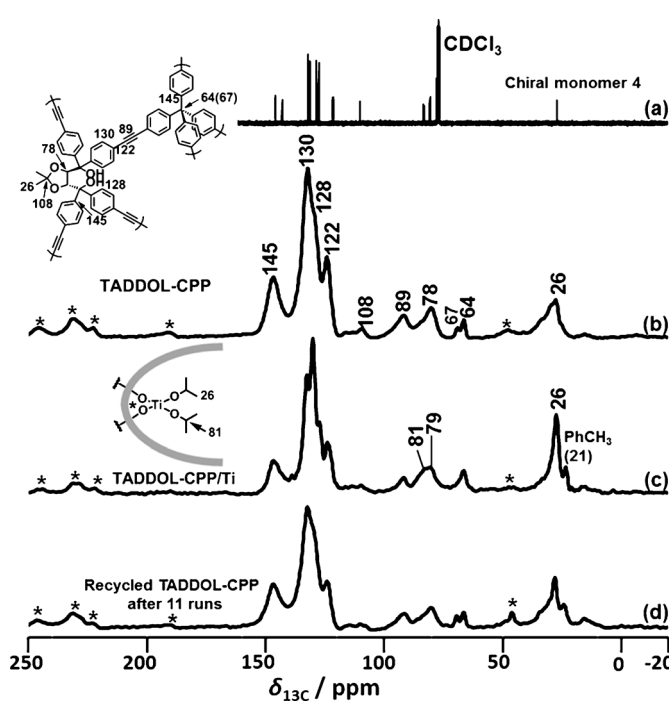
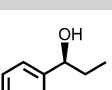


Figure 1. The liquid ¹³C NMR spectrum (CDCl₃, 100 MHz) of the chiral monomer **4** (a), and the solid-state ¹³C CP/MAS NMR (100 MHz) spectra of **TADDOL-CPP** (b), **TADDOL-CPP/Ti** (c), and the recycled **TADDOL-CPP** after the 11th run (d). The asterisks denote the spinning sidebands. The ¹³C NMR signal at $\delta=21$ ppm is due to the residual toluene.

Catalytic performance of **TADDOL-CPP**

We then explored the catalytic activity of **TADDOL-CPP**. As it is well known, the asymmetric addition of Et₂Zn to aldehydes provides a feasible approach to the synthesis of optically pure secondary alcohols that are among the most important intermediates in the pharmaceutical synthesis.^[53] The research on homogeneous systems has proposed that the dihydroxy groups of TADDOLs^[34] can easily coordinate with Ti^{IV} and the obtained cooperative catalysts are essential for the asymmetric addition of Et₂Zn to aldehydes. Accordingly, we used **TADDOL-CPP** as the asymmetric heterogeneous catalyst in the addition reaction of Et₂Zn to aldehydes. We found that, in the presence of [Ti(O*i*Pr)₄], **TADDOL-CPP** presented excellent enantioselective control (84–94% ee) to a variety of aldehyde substrates.

Table 1. Optimization of the reaction conditions for the asymmetric addition of Et₂Zn to benzaldehyde catalyzed by **TADDOL-CPP** in the presence of [Ti(O*i*Pr)₄].^[a]

| Entry | Catalyst [mol %] | [Ti(O <i>i</i> Pr) ₄] [equiv] | T [°C] | Yield ^[b] [%] | ee ^[c] [%] |  | |
|-------------------|---------------------|--|-----------|-----------------------------|--------------------------|---|--|
| | | | | | | | |
| 1 | TADDOL-CPP (10) | 1.7 | -30 | 77 | 88 | | |
| 2 | TADDOL-CPP (20) | 1.7 | -30 | 78 | 91 | | |
| 3 | TADDOL-CPP (30) | 1.7 | -30 | 74 | 90 | | |
| 4 | TADDOL-CPP (20) | 1.7 | -40 | 79 | 91 | | |
| 5 | TADDOL-CPP (20) | 1.7 | -20 | 73 | 89 | | |
| 6 | TADDOL-CPP (20) | 2.0 | -30 | 86 | 91 | | |
| 7 | TADDOL-CPP (20) | 2.3 | -30 | 80 | 91 | | |
| 8 ^[d] | - | - | -30 | trace | - | | |
| 9 ^[e] | - | 2.0 | -30 | 58 | 0 | | |
| 10 ^[f] | TADDOL-CPP (20) | - | -30 | 18 | 0 | | |
| 11 ^[g] | TADDOL-CPP/Ti (20) | - | -30 | 21 | 36 | | |
| 12 ^[g] | TADDOL-CPP/Ti (20) | 1.8 | -30 | 81 | 90 | | |
| 13 ^[h] | 3 (20) | 2.0 | -30 | 93 (79 ^[i]) | 96 | | |

[a] General conditions: Benzaldehyde (0.19 mmol), Et₂Zn (0.57 mmol), anhydrous toluene (1.3 mL), 48 h. **TADDOL-CPP** (or 3) and [Ti(O*i*Pr)₄] served as the cooperative catalyst. [b] Yield of the isolated product. [c] Determined by chiral HPLC (Daicel chiral OD-H column). The absolute configuration of the product was determined according to the references.^[35,54] [d] The reaction without any catalyst. [e] [Ti(O*i*Pr)₄] alone was used as the catalyst. [f] **TADDOL-CPP** alone was used as the heterogeneous catalyst. [g] The isolated **TADDOL-CPP/Ti** was used as the heterogeneous catalyst. [h] The homogeneous counterpart 3 and [Ti(O*i*Pr)₄] were used as the cooperative catalyst. [i] Yield for the reaction catalyzed by 3 in 24 h.

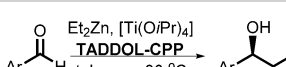
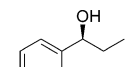
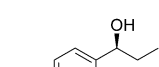
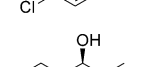
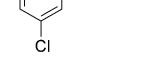
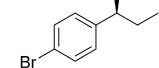
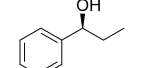
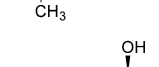
Moreover, the control experiments verified the cooperative catalysis contribution from both **TADDOL-CPP** and [Ti(O*i*Pr)₄].

We first examined the catalytic activity of **TADDOL-CPP** in asymmetric addition of Et₂Zn to benzaldehyde (Table 1). In the presence of 10 mol % of **TADDOL-CPP** and 1.7 equiv of [Ti(O*i*Pr)₄], the reaction proceeded smoothly in toluene at -30 °C (Table 1, entry 1), producing the desired chiral secondary alcohol in good yield (77 %) and with a high ee value (88 %). The ee value could be further enhanced to 91 % when the loading of **TADDOL-CPP** was increased to 20 mol % (Table 1, entry 2). Further increase of the **TADDOL-CPP** loading to 30 mol % resulted in, however, a similar yield and ee value (Table 1, entry 3). Investigation on the influence of the reaction temperature revealed that -30 °C was appropriate for the reaction (Table 1, entries 2, 4, and 5). As reported by Gau et al.,^[55] an appropriate increase in the amount of [Ti(O*i*Pr)₄] could reduce the side reactions. Consequently, an improved yield (86 %, Table 1, entry 6) was achieved by using 2.0 equiv of [Ti(O*i*Pr)₄] relative to benzaldehyde. Importantly, control experiments further showed that the reaction could not proceed in the absence of the catalysts (Table 1, entry 8). Moreover, [Ti(O*i*Pr)₄] alone could catalyze this addition reaction (58 % yield) but with no enantioselectivity (Table 1, entry 9). These results demonstrated the cooperativity of the catalysts: [Ti(O*i*Pr)₄] is necessary for binding and activating the substrates, whereas **TADDOL-CPP** is responsible for the enantioselective control. By recognizing the cooperative nature of the working catalysts, the optimal reaction

condition for the asymmetric addition of Et₂Zn to aromatic aldehydes was then chosen to be 20 mol % of **TADDOL-CPP** with 2.0 equiv of [Ti(O*i*Pr)₄] at a reaction temperature of -30 °C. For the purpose of comparison, the chiral monomer 3 was also applied to catalyze the same reaction. The catalytic results (Table 1, entry 13) showed that **TADDOL-CPP** possesses the comparable activity (reaction in 48 h) as its homogeneous counterpart 3 (reaction in 24 h).

After establishing the optimal reaction condition, we next examined the substrate scope for this reaction. As revealed in Table 2, a wide range of aromatic aldehydes with either the

Table 2. Asymmetric addition of Et₂Zn to aromatic aldehydes catalyzed by **TADDOL-CPP** in the presence of [Ti(O*i*Pr)₄].^[a]

| Entry | Product | Yield ^[b] [%] | ee ^[c] [%] |  | |
|-------|--|-----------------------------|--------------------------|--|--|
| | | | | | |
| 1 |  | 86 | 91 | | |
| 2 |  | 95 | 88 | | |
| 3 |  | 90 | 92 | | |
| 4 |  | 92 | 91 | | |
| 5 |  | 96 | 84 | | |
| 6 |  | 92 | 90 | | |
| 7 |  | 96 | 94 | | |

[a] General conditions: aromatic aldehydes (0.19 mmol), **TADDOL-CPP** (0.038 mmol), [Ti(O*i*Pr)₄] (0.38 mmol), Et₂Zn (0.57 mmol), anhydrous toluene (1.3 mL), 48 h. **TADDOL-CPP** and [Ti(O*i*Pr)₄] served as the cooperative catalyst. [b] Yield of the isolated product. [c] Determined by chiral HPLC.

electron-withdrawing or electron-donating substituents on the benzene ring are well applicable (Table 2, entries 1–7), producing the chiral secondary alcohols in excellent yields (86–96 %) and with high ee values (84–94 %). The electronic feature and the substituent position (*meta* or *para*) on the benzene ring exhibited only a slight effect on the stereoselectivity of the reaction products. Compared with benzaldehyde, the 2-naph-

thaldehyde substrate showed even better results, producing the corresponding product in 96% yield and with 94% *ee* (Table 2, entry 7).

Catalytic mechanism of TADDOL-CPP

In accordance with those found^[57] for the homogeneous systems, our results (Table 1, entries 6–12) have shown the clear evidence for the cooperative catalysis of TADDOL-CPP and $[\text{Ti}(\text{O}i\text{Pr})_4]$. To gain further insights into the reaction mechanism, we prepared the cooperative TADDOL-CPP/Ti catalyst through a post-treatment^[34] of TADDOL-CPP with $[\text{Ti}(\text{O}i\text{Pr})_4]$ (Scheme 1). The obtained TADDOL-CPP/Ti catalyst was then subject to characterization. As shown in the ^{13}C CP/MAS NMR spectrum (Figure 1c), the increased signal at $\delta = 26$ ppm and the new signal at $\delta = 81$ ppm originate from the carbon atoms of the isopropoxy groups in TADDOL-CPP/Ti. The chemical shifts of other ^{13}C NMR signals for TADDOL-CPP/Ti (Figure 1c) remain unchanged as those for TADDOL-CPP (Figure 1b). Compared with TADDOL-CPP, TADDOL-CPP/Ti exhibits a slightly lower thermal stability, as revealed by the TGA measurement (the Supporting Information, Figure S1). The inductively coupled plasma (ICP) analysis indicated that the Ti content in TADDOL-CPP/Ti was 3.0%, which is in consistent with the calculated value (3.8%). Energy-dispersive X-ray spectroscopic (EDX) analysis also afforded evidence for the existence of the titanium species (the Supporting Information, Figure S6). As shown in the SEM and TEM images (the Supporting Information, Figure S4 and S5), the morphology of TADDOL-CPP/Ti is similar to that of TADDOL-CPP. In addition, the measured BET surface area of TADDOL-CPP/Ti is $579 \text{ m}^2 \text{ g}^{-1}$. All these information indicated that the Ti^{IV} species has successfully been chelated within the TADDOL-CPP polymeric network, and the porous structure of TADDOL-CPP was well maintained during the post-modification with $[\text{Ti}(\text{O}i\text{Pr})_4]$. As expected, the TADDOL-CPP/Ti catalyst showed excellent catalytic performance in the enantiocontrol (Table 1, entries 9–12). These results once again confirmed the cooperativity of TADDOL-CPP/Ti: $[\text{Ti}(\text{O}i\text{Pr})_4]$ for the substrate activation and TADDOL-CPP for the enantioselective control.

We propose herein a possible reaction mechanism (Figure 2) for the heterogeneous asymmetric addition catalyzed by TADDOL-CPP/ $[\text{Ti}(\text{O}i\text{Pr})_4]$ based on our observation and those from the homogeneous systems.^[57] Initially, the ethyl group of Et_2Zn and the isopropoxy group of TADDOL-CPP/Ti exchange with each other^[57a] to produce a primary intermediate A. The benzaldehyde substrate can be fixed through the $\text{Ti}^{IV}\cdots\text{O}=\text{C}-$ interaction and activated upon the Ti^{IV} active sites of A, through which the enantioselectivity can be controlled and the chiral intermediate B is formed. The intermediate B can be converted back to A or reacted further to D through the exchange reactions. Meanwhile, the excess of $[\text{Ti}(\text{O}i\text{Pr})_4]$ will recover TADDOL-CPP/Ti from B or D to produce E, and consequently, promote the catalytic cycle.^[57a] Thus, the reaction could proceed efficiently in this TADDOL-based catalytic system. Finally, when treated with the saturated NH_4Cl solution, the intermediates C or E can be further converted to the corresponding chiral secondary alcohols.

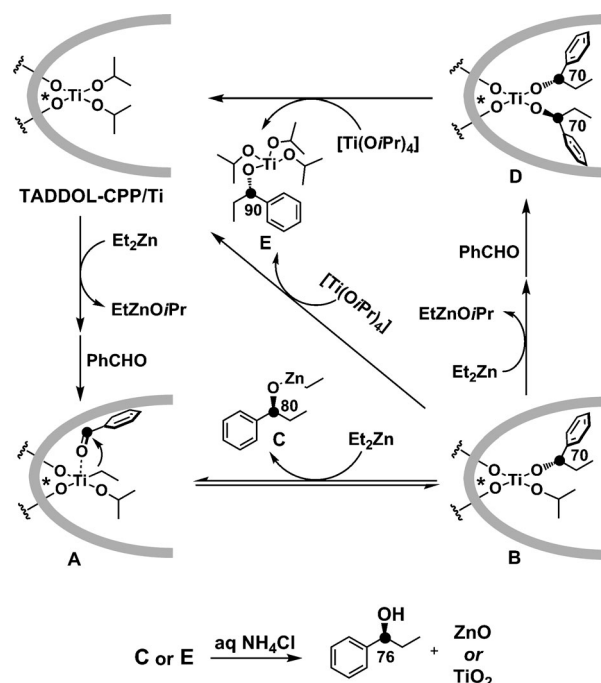


Figure 2. The reaction mechanism proposed for the asymmetric addition of Et_2Zn to aromatic aldehydes (PhCHO as an example) catalyzed by TADDOL-CPP/ $[\text{Ti}(\text{O}i\text{Pr})_4]$. The deactivation of catalyst could be caused by the formed metallic oxides and the residual organic species occluded into the pores of the working catalyst. The ^{13}C chemical shifts of the marked (●) atoms are indicated.

or E can be further converted to the corresponding chiral secondary alcohols.

The proposed mechanism (Figure 2) was further verified by our ^{13}C NMR spectroscopic observation of the intermediates B (or D), C, and E on TADDOL-CPP/Ti. For this purpose, the selectively ^{13}C -labeled Ph^{13}CHO (see the Supporting Information for its synthesis and characterization) was used as the substrate, and the catalytic process was directly monitored with solid-state ^{13}C CP/MAS NMR spectroscopy. Compared with that of the blank TADDOL-CPP/Ti catalyst (Figure 1c), the NMR spectra (Figure 3) of the working TADDOL-CPP/Ti catalysts showed a significant difference, demonstrating the transformation of ^{13}C -labeled Ph^{13}CHO . For clarity, the new signals are marked as “▼” in Figure 3. In Figure 3a is shown the ^{13}C CP/MAS NMR spectrum recorded for the transformation of Ph^{13}CHO on TADDOL-CPP/Ti (reaction condition as in Table 1, entry 12). The new signals at $\delta = 80$ and 90 ppm are attributed to the intermediates C and E, respectively. These assignments have been supported by liquid ^{13}C NMR data: We synthesized the intermediates C and E, which indeed showed the liquid ^{13}C NMR signals at $\delta = 82$ and 88 ppm, respectively (the Supporting Information, Figure S10). In addition, the supernatant after the heterogeneous reaction showed the liquid ^{13}C NMR signals at $\delta = 82$ and 88 ppm as well (the Supporting Information, Figure S11). Furthermore, adsorption of C and E on TADDOL-CPP resulted in the ^{13}C CP/MAS NMR signals at $\delta = 80$ and 90 ppm, respectively (the Supporting Information, Figure S12). All these data verified the existence of the intermediates C and E.

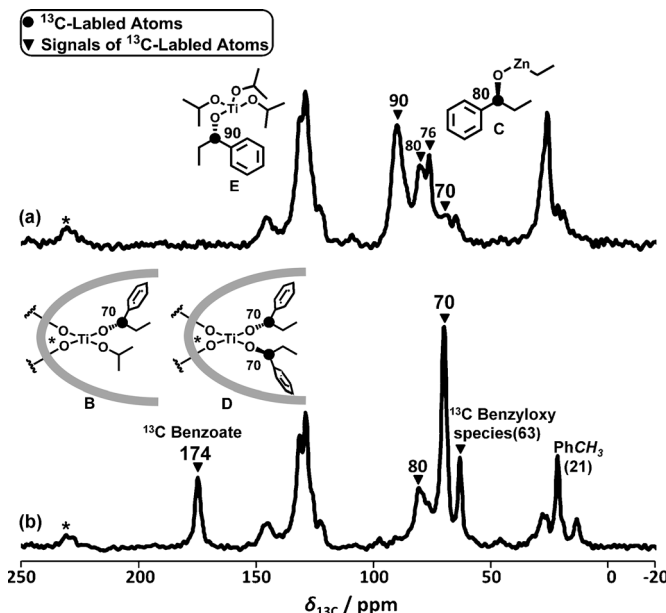


Figure 3. Solid-state ^{13}C CP/MAS NMR (100 MHz) spectra of the **TADDOL-CPP/Ti** catalyst for the reaction of Et_2Zn and Ph^{13}CHO with (a) and without (b) the adding of additional $[\text{Ti}(\text{O}i\text{Pr})_4]$. The asterisks denote the spinning sidebands. The ^{13}C -labeled atoms are marked as (●), and their ^{13}C NMR chemical shifts are indicated. Unmarked signals are due to the carbon atoms on the blank **TADDOL-CPP/Ti** catalyst (see Figure 1c).

ates **C** and **E** on **TADDOL-CPP/Ti** catalyst, through which the catalytic cycle in Figure 2 can be validated.

The additional signal at $\delta = 70$ ppm in Figure 3a should originate from the surface species **B** (or **D**, their chemical shifts cannot be distinguished). Without the addition of the excess $[\text{Ti}(\text{O}i\text{Pr})_4]$ (reaction condition as in Table 1, entry 11), the signal at $\delta = 70$ ppm dominates the corresponding ^{13}C CP/MAS NMR spectrum (Figure 3b). The difference between Figure 3a and 3b accordingly highlights the role for the excess $[\text{Ti}(\text{O}i\text{Pr})_4]$: The surface species **B** and **D** can be further transformed upon reaction with $[\text{Ti}(\text{O}i\text{Pr})_4]$, which promotes the catalytic cycle shown in Figure 2. Besides, the signals at $\delta = 63$ and 174 ppm in Figure 3b are characteristics of ^{13}C -benzyloxy and -benzoate species, both of which come from the side reactions of Ph^{13}CHO .^[58] These two signals are absent in Figure 3a, implying that the excess $[\text{Ti}(\text{O}i\text{Pr})_4]$ could suppress the side reactions.^[57a] It is worth mentioning that, by ^{13}C liquid and solid-state NMR spectroscopy, we have identified the key intermediates formed in the reaction of diethylzinc to aromatic aldehydes. This information has never been obtained before in any other homogeneous or heterogeneous systems.

The mechanism proposed in Figure 2, however, has not considered the contribution from the inherent pores of the **TADDOL-CPP** catalyst. Additional control experiments showed that the enantioselectivity of the reaction products was affected by the size of the polycyclic aromatic aldehydes: the larger substrate gave the lower ee value (Table 3, entries 1–3). Compared with **TADDOL-CPP**, the homogeneous counterpart **3** showed better enantioselectivity when catalyzing the same bulky aldehydes (data shown in the parentheses, Table 3, en-

Table 3. Asymmetric addition of Et_2Zn to aromatic aldehydes catalyzed by **TADDOL-CPP** or **3** in the presence of $[\text{Ti}(\text{O}i\text{Pr})_4]$.^[a]

| Entry | Product | Yield ^[b] [%] | ee ^[c] [%] |
|-------|---------|-----------------------------|--------------------------|
| 1 | | 96 (99 ^[d]) | 94 (99 ^[d]) |
| 2 | | 84 (95 ^[d]) | 74 (93 ^[d]) |
| 3 | | 91 (88 ^[d]) | 65 (86 ^[d]) |

[a] General conditions: aromatic aldehydes (0.19 mmol), **TADDOL-CPP** (or **3**) (0.038 mmol), $[\text{Ti}(\text{O}i\text{Pr})_4]$ (0.38 mmol), Et_2Zn (0.57 mmol), anhydrous toluene (1.3 mL), 48 h. **TADDOL-CPP** (or **3**) and $[\text{Ti}(\text{O}i\text{Pr})_4]$ served as the cooperative catalyst. [b] Yield of the isolated product. [c] Determined by chiral HPLC. [d] For the purpose of comparison, compound **3** and $[\text{Ti}(\text{O}i\text{Pr})_4]$ were used as the cooperative catalyst and the obtained results are presented in parentheses.

tries 1–3). These results imply that, in addition to the local chiral environment, the nanopores (together with the pore walls) of **TADDOL-CPP** should have further impacts on the enantioselectivity. Therefore, only the aldehyde substrates with suitable size that matches well with the microporous dimensions of **TADDOL-CPP** could possibly achieve a higher ee value. In this context, the large mesopores may mainly offer an access to the catalytic sites and promote the mass transport process. In fact, the hierarchical structures containing both micropores and mesopores have long been pursued in inorganic zeolites as a key solution to improving the catalytic performance.^[32] The same concept has been applied therein: The micropores in the hierarchical zeolites govern the shape-selective catalysis, whereas the mesopores (or macropores) improve the site accessibility and molecular transport.

Recyclability and deactivation mechanism of **TADDOL-CPP**

Finally, we evaluated the stability and recyclability of **TADDOL-CPP**. The recycling experiments were carried out with the asymmetric addition of Et_2Zn to benzaldehyde under the optimal reaction conditions as in Table 1, entry 6. Compared with **JH-CPP**,^[22] an efficient heterogeneous organocatalyst for the asymmetric Michael addition reaction, **TADDOL-CPP** showed remarkable enhancement in the recyclability and catalytic stability. As shown in Figure 4, **TADDOL-CPP** can be reused for at least 11 iterative runs without an obvious loss of activity (yield from 86 to 77%; however, the ee value decreases from 91 to 76%). The ^{13}C CP/MAS NMR spectrum recorded for the catalyst used after the 11th run revealed that the spectral features of

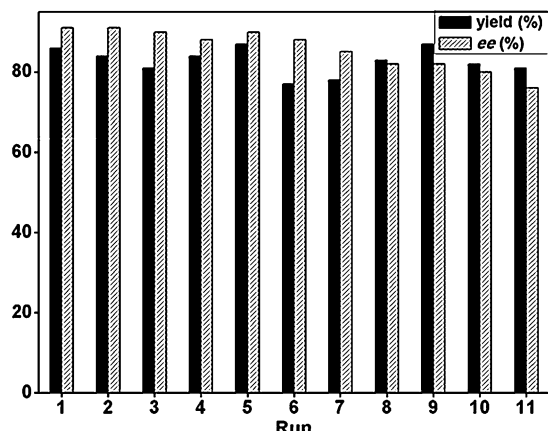


Figure 4. Evaluation of the recyclability of **TADDOL-CPP** in the asymmetric addition of Et_2Zn to benzaldehyde. All the recycling experiments reactions (runs 2 to 11) were carried out for 48 h with benzaldehyde (0.19 mmol) under identical condition as in Table 1, entry 6. The yield of the isolated product is given for each run.

TADDOL-CPP were well maintained (Figure 1d), indicating that the **TADDOL-CPP** network is robust for recycling and reuse. Upon the repeated recycling, the micropores in **TADDOL-CPP** may gradually capture the guest molecules (e.g., the residual products, unreacted substrates, and so on). Indeed, the ^{13}C CP/MAS NMR spectrum recorded for the recycled **TADDOL-CPP** after the 11th run showed small changes in the high-field region ($\delta = 0$ to 50 ppm, Figure 1d), implying the inclusion of bulky organic species. Meanwhile, the increased Ti content (4.4%) identified by the ICP analysis of **TADDOL-CPP** after the 11th run also suggested the formation of inorganic titanium oxide species (TiO_2). Indeed, liberation from the organic metal species has been suggested as the origin for the formation of metal oxides (Figure 2).^[34,47] The BET surface area and the total volume of the recycled **TADDOL-CPP** catalyst after the 6th run were decreased to $421 \text{ m}^2 \text{ g}^{-1}$ and $0.29 \text{ cm}^3 \text{ g}^{-1}$, respectively (the Supporting Information, Figure S8b). Further decrease of the BET surface area to $148 \text{ m}^2 \text{ g}^{-1}$ and of the total volume to $0.09 \text{ cm}^3 \text{ g}^{-1}$ was found for the recycled **TADDOL-CPP** after the 11th run (the Supporting Information, Figure S8c). Gradual decrease in the enantioselectivity could therefore attribute to the diminished BET surface area and the total volume. It emphasizes again the importance of the porous structure for the catalytic performance of **TADDOL-CPP**. Accordingly, instead of the decomposition of **TADDOL-CPP** network, the residual bulky organic species and the metallic oxides (TiO_2 or ZnO) occluded within the pores should be the main reasons for the deactivation of the **TADDOL-CPP** catalyst.

Discussion on the structure–property–activity relationship

Exploration of the POP materials for heterogeneous catalysis is a new research topic and, thus, very little information is available for the application-oriented synthesis of highly efficient POP catalysts. Particularly, for the designed construction of chiral POPs, an excellent enantioselective performance should be considered as the first priority in addition to the require-

ments for the diastereoselectivity and the reaction yield. For this purpose, we first synthesized chiral **TADDOL-CPP** catalyst through a concise three-step route (Scheme 1). The catalytic reactions under different conditions and with different substrates not only identified the cooperative nature of the working catalyst but also improved our understanding on the structure–activity relationship. The key information obtained is summarized as follows.

Design principle

The first prerequisites for reaching an excellent performance in asymmetric catalysis are rational design and concise synthesis of the chiral catalyst itself. Similar for the homogeneous or immobilized catalysts, the rational design for the chiral POP catalysts should at least include the concerns of the binding (active) site and the chiral environment: The binding site would anchor the substrates upon activation and the chiral environment could adjust the orientation of substrates upon reaction. Under the optimal reaction conditions, the cooperative nature between binding site and chiral environment should bring about the best enantiocontrol. In this study, the Ti^{IV} center serves as a binding site and the **TADDOL-CPP** network offers the chiral environment (Figure 2). The cooperative catalysis has well been evidenced by the catalytic results (Table 1, entries 6–12). In addition, the construction of permanent porous structure is key to ensure the accessibility of the active sites and facilitate the mass transport. To improve the BET surface area and the pore volume of **TADDOL-CPP**, three-dimensional rigid monomers **4** and **5** were selected as the functional and structural monomers, respectively. The reproducibility for synthesis of porous catalysts and for their catalytic activity much relies on the rigidity of building blocks and on the precise control of the reaction conditions.

Uniform distribution of the catalytic sites

Facilely constructed through the covalent bonding of rigid monomers, the porous **TADDOL-CPP** is robust and uniformly embedded with accessible dihydroxy groups. Lin and co-workers recently reported the use of 1,1'-binaphthyl-embedded cross-linked polymer/Ti (denoted as CCP/Ti) as a Lewis acid catalyst to promote asymmetric addition of Et_2Zn to aldehydes.^[20] The CCP/Ti catalyst could afford the alcohol products in quantitative yields but with only modest ee values (55–81%). They proposed that the low ee values could be attributed to the formation of intermolecular $[(\text{O}i\text{Pr})_2\text{Ti}(\text{BINOL})_2]$ ($\text{BINOL} = 1,1'\text{-bi-2-naphthol}$) binary complexes upon the further reaction of $[\text{Ti}(\text{O}i\text{Pr})_4]$.^[20,56] Because the **TADDOL** moieties in **TADDOL-CPP** were evenly separated by the bulky 3D structural units, the simultaneous interaction of $[\text{Ti}(\text{O}i\text{Pr})_4]$ with two **TADDOL** moieties to form the similar binary complexes could be prevented. As a result, excellent ee values were obtained in our case.

Local "chiral pocket"

The unique structure in **TADDOL-CPP** offers an ideal chiral environment for enantiocontrol. We were able to obtain the single crystals of monomer **4** (the Supporting Information). The X-ray single-crystal structure of **4** (Scheme 1) shows that, the four benzene rings are arranged like rigid butterfly wings, which could offer the steric shielding. The bulky benzene rings in the network of **TADDOL-CPP** has afforded the local "chiral pocket".^[31] The best orientation for reaction substrates could be reached within this "chiral pocket", which ensures the high stereoselectivity of the products. The importance of this "chiral pocket" was also verified by the excellent performance of the homogeneous catalyst **3** (Table 1, entry 13).

Hierarchical porous structure

For the porous catalytic systems, a key question to answer is whether the catalysis being performed within the pores or on the outer surface. It is quite clear in this study that the asymmetric heterogeneous catalysis takes place within the **TADDOL-CPP** nanopores as well. Firstly, **TADDOL-CPP** and its homogeneous counterpart **3** showed comparable activity for the smaller substrates but showed difference for the bulky ones. Secondly, the partial blocking of the nanopores in the recycled **TADDOL-CPP** catalyst resulted in the slight decrease of the catalyst activity (Figure 4).

Conclusion

Recent years have witnessed a rapid development in the new research area of POP materials. Towards the practical application of functional POPs in asymmetric heterogeneous catalysis, we achieved herein a concise construction of a TADDOL-derived chiral POP catalyst, **TADDOL-CPP**, and investigated its structure–property–activity relationship in catalyzing the asymmetric addition reaction of Et₂Zn to aromatic aldehydes. The main results obtained are summarized in the following:

- 1) For the first time,^[23c] the TADDOL moiety was used as the functional building block for the convenient construction of the chiral POP catalyst. Through a concise "bottom-up" strategy shown in Scheme 1, **TADDOL-CPP** can be reproducibly synthesized within three steps from readily available building blocks. Due to the efficient covalent linkages between the rigid three-dimensional building blocks, **TADDOL-CPP** possesses the porous structure, high BET surface area, and enhanced stability. Meanwhile, the TADDOL moieties are evenly distributed in the network.
- 2) As shown in the X-ray single-crystal structure of **4**, the local "chiral pocket" is constructed from the rigid benzene rings, providing **TADDOL-CPP** with an ideal chiral environment for the enantiocontrol. Meanwhile, the hierarchical porous structure may offer additional benefits for the catalytic performance of **TADDOL-CPP**: The micropores provide the confined space for enantiocontrol and the mesopores facilitate mass transport. As a result, **TADDOL-CPP** exhibited an

excellent asymmetric catalytic activity (up to 94% ee) in asymmetric addition reaction of Et₂Zn to aromatic aldehydes. Meanwhile, beneficial from the rigid and hierarchical porous structure with abundant mesopores, **TADDOL-CPP** could be easily recovered and reused for at least 11 iterative cycles without a significant loss of its catalytic activity.

- 3) In an effort to offer further insights on the designed synthesis of the robust POP catalysts, we studied the reaction mechanism involved in the chiral POP catalysis. By using solid-state ¹³C MAS NMR spectroscopy, we observed directly the key intermediates formed upon the reaction of ¹³C-labeled benzaldehyde reactant on the catalyst. The porous structure has ensured the formation of these intermediates in a large amount so that the direct ¹³C NMR spectroscopic observation is feasible. Meanwhile, we found the key parameters (such as the building blocks, cooperative catalysis, local chiral environment, and hierarchical porous structure) that affect the catalytic performance of **TADDOL-CPP**.

With the excellent activity and recyclability, the easily prepared **TADDOL-CPP** catalyst may have further applications in the industrial production of chiral secondary alcohols. Moreover, **TADDOL-CPP** may also be used as an efficient heterogeneous catalyst to promote various asymmetric reactions, such as the Diels–Alder and Mukaiyama–aldol reactions. Besides, as a good H-bond donor, **TADDOL-CPP** could also work as a new candidate for the stationary phases of HPLC or GC for the enantiomer separation.^[34] Furthermore, we expect that the mechanism-related information offered herein may shed new light on the designed synthesis of robust POP catalysts.

Acknowledgements

Financial support from the National Natural Science Foundation of China (No. 21172103), the 111 project, the Innovative Research Team in University (PCSIRT: IRT1138), and the Fundamental Research Funds for the Central Universities (Izujbky-2013-ct02) is gratefully acknowledged. We thank Prof. Wei Yu at Lanzhou University for the valuable comments.

Keywords: chirality • heterogeneous catalysis • NMR spectroscopy • polymers • reaction mechanisms • structure–activity relationships

[1] a) J.-X. Jiang, F. Su, A. Trewin, C. D. Wood, N. L. Campbell, H. Niu, C. Dickinson, A. Y. Ganin, M. J. Rosseinsky, Y. Z. Khimyak, A. I. Cooper, *Angew. Chem.* **2007**, *119*, 8728–8732; *Angew. Chem. Int. Ed.* **2007**, *46*, 8574–8578; b) J.-X. Jiang, F. Su, A. Trewin, C. D. Wood, H. Niu, J. T. A. Jones, Y. Z. Khimyak, A. I. Cooper, *J. Am. Chem. Soc.* **2008**, *130*, 7710–7720.

[2] a) P. Kuhn, A. Forget, D. S. Su, A. Thomas, M. Antonietti, *J. Am. Chem. Soc.* **2008**, *130*, 13333–13337; b) M. G. Schwab, B. Fassbender, H. W. Spiess, A. Thomas, X. L. Feng, K. Mullen, *J. Am. Chem. Soc.* **2009**, *131*, 7216–7217.

[3] a) N. B. McKeown, P. M. Budd, *Macromolecules* **2010**, *43*, 5163–5176.

[4] a) A. I. Cooper, *Adv. Mater.* **2009**, *21*, 1291–1295; b) J.-X. Jiang, A. I. Cooper, *Top. Curr. Chem.* **2009**, *293*, 1–33.

- [5] a) A. Thomas, P. Kuhn, J. Weber, M.-M. Titirici, M. Antonietti, *Macromol. Rapid Commun.* **2009**, *30*, 221–236; b) A. Thomas, *Angew. Chem. Int. Ed.* **2010**, *49*, 8328–8344.
- [6] J. Germain, J. M. J. Fréchet, F. Svec, *Small* **2009**, *5*, 1098–1111.
- [7] D. Wu, F. Xu, B. Sun, R. Fu, H. He, K. Matyjaszewski, *Chem. Rev.* **2012**, *112*, 3959–4015.
- [8] a) L. E. Kreno, K. Leong, O. K. Farha, M. Allendorf, R. P. Van Duyne, J. T. Hupp, *Chem. Rev.* **2012**, *112*, 1105–1125; b) N. Stock, S. Biswas, *Chem. Rev.* **2012**, *112*, 933–969; c) S. M. Cohen, *Chem. Rev.* **2012**, *112*, 970–1000.
- [9] a) X. Feng, X. Ding, D. Jiang, *Chem. Soc. Rev.* **2012**, *41*, 6010–6022; b) Y. Xu, S. Jin, H. Xu, A. Nagai, D. Jiang, *Chem. Soc. Rev.* **2013**, *42*, 8012–8031.
- [10] S.-Y. Ding, W. Wang, *Chem. Soc. Rev.* **2013**, *42*, 548–568.
- [11] a) S. Xu, Y. Luo, B. Tan, *Macromol. Rapid Commun.* **2013**, *34*, 471–484; b) Z. Chang, D.-S. Zhang, Q. Chen, X.-H. Bu, *Phys. Chem. Chem. Phys.* **2013**, *15*, 5430–5442.
- [12] For selected examples of POPs on gas storage, see: a) J. Germain, F. Svec, J. M. J. Fréchet, *Chem. Mater.* **2008**, *20*, 7069–7076; b) T. Ben, H. Ren, S. Ma, D. Cao, J. Lan, X. Jing, W. Wang, J. Xu, F. Deng, J. M. Simmons, S. Qiu, G. Zhu, *Angew. Chem.* **2009**, *121*, 9621–9624; *Angew. Chem. Int. Ed.* **2009**, *48*, 9457–9460; c) O. K. Farha, Y.-S. Bae, B.G. Hauser, A.M. Spokoyny, R.Q. Snurr, C.A. Mirkin, J.T. Hupp, *Chem. Commun.* **2010**, *46*, 1056–1058; d) Q. Chen, J.-X. Wang, Q. Wang, N. Bian, Z.-H. Li, C.-G. Yan, B.-H. Han, *Macromolecules* **2011**, *44*, 5573–5577; e) D. Yuan, W. Lu, D. Zhao, H.-C. Zhou, *Adv. Mater.* **2011**, *23*, 3723–3725; f) M. H. Weston, O. K. Farha, B. G. Hauser, J. T. Hupp, S. T. Nguyen, *Chem. Mater.* **2012**, *24*, 1292–1296; g) Y. Zhu, H. Long, W. Zhang, *Chem. Mater.* **2013**, *25*, 1630–1635.
- [13] For selected examples of POPs on gas separation, see: a) O. K. Farha, A. M. Spokoyny, B. G. Hauser, Y.-S. Bae, S. E. Brown, R. Q. Snurr, C. A. Mirkin, J. T. Hupp, *Chem. Mater.* **2009**, *21*, 3033–3035; b) W. Lu, D. Yuan, J. Sculley, D. Zhao, R. Krishna, H.-C. Zhou, *J. Am. Chem. Soc.* **2011**, *133*, 18126–18129; c) Q. Chen, M. Luo, P. Hammershoj, D. Zhou, Y. Han, B. W. Laursen, C.-G. Yan, B.-H. Han, *J. Am. Chem. Soc.* **2012**, *134*, 6084–6087; d) Y. Luo, B. Li, W. Wang, K. Wu, B. Tan, *Adv. Mater.* **2012**, *24*, 5703–5707; e) M. H. Weston, G. W. Peterson, M. A. Browne, P. Jones, O. K. Farha, J. T. Hupp, S. T. Nguyen, *Chem. Commun.* **2013**, *49*, 2995–2997; f) L. Xie, M. P. Suh, *Chem. Eur. J.* **2013**, *19*, 11590–11597; g) H. A. Patel, S. H. Je, J. Park, D. P. Chen, Y. Jung, C. T. Yavuz, A. Coskun, *Nat. Commun.* **2013**, *4*, 1357.
- [14] L. Chen, Y. Honsho, S. Seki, D. Jiang, *J. Am. Chem. Soc.* **2010**, *132*, 6742–6748.
- [15] For selected examples of POPs on molecular recognition/sensors, see: a) N. A. Rakow, M. S. Wendland, J. E. Trend, R. J. Poirier, D. M. Paolucci, S. P. Maki, C. S. Lyons, M. J. Swierczek, *Langmuir* **2010**, *26*, 3767–3770; b) X. Liu, Y. Xu, D. Jiang, *J. Am. Chem. Soc.* **2012**, *134*, 8738–8741; c) Z. Xiang, D. Cao, *Macromol. Rapid Commun.* **2012**, *33*, 1184–1190; d) J. L. Novotney, W. R. Dichtel, *ACS Macro Lett.* **2013**, *2*, 423–426; e) K. Wu, J. Guo, C. Wang, *Chem. Commun.* **2014**, *50*, 695–697; f) J. Liu, K.-K. Yee, K. K.-W. Lo, K. Y. Zhang, W.-P. To, C.-M. Che, Z. Xu, *J. Am. Chem. Soc.* **2014**, *136*, 2818–2824.
- [16] a) P. Kaur, J. T. Hupp, S. T. Nguyen, *ACS Catal.* **2011**, *1*, 819–835; b) R. Dawson, A. I. Cooper, D. J. Adams, *Prog. Polym. Sci.* **2012**, *37*, 530–563; c) Y. Zhang, S. N. Riduan, *Chem. Soc. Rev.* **2012**, *41*, 2083–2094.
- [17] For selected examples of POPs on heterogeneous catalysis with metals, see: a) L. M. Bronstein, G. Goerigk, M. Kostylev, M. Pink, I. A. Khotina, P. M. Valetsky, V. G. Matveeva, E. M. Sulman, M. G. Sulman, A. V. Bykov, N. V. Lakina, R. J. Spontak, *J. Phys. Chem. B* **2004**, *108*, 18234–18242; b) H. J. Mackintosh, P. M. Budd, N. B. McKeown, *J. Mater. Chem.* **2008**, *18*, 573–578; c) C. D. Wood, B. Tan, A. Trewin, F. Su, M. J. Rosseinsky, D. Bradshaw, Y. Sun, L. Zhou, A. I. Cooper, *Advanced Materials* **2008**, *20*, 1916–1921; d) Y. Zhang, S. N. Riduan, J. Y. Ying, *Chem. Eur. J.* **2009**, *15*, 1077–1081; e) S. Makhseed, F. Al-Kharafi, J. Samuel, B. Ateya, *Catal. Commun.* **2009**, *10*, 1284–1287; f) R. Palkovits, M. Antonietti, P. Kuhn, A. Thomas, F. Schüth, *Angew. Chem.* **2009**, *121*, 7042–7045; *Angew. Chem. Int. Ed.* **2009**, *48*, 6909–6912; g) C. E. Chan-Thaw, A. Villa, P. Katekomol, D. Su, A. Thomas, L. Prati, *Nano Lett.* **2010**, *10*, 537–541; h) L. Chen, Y. Yang, D. Jiang, *J. Am. Chem. Soc.* **2010**, *132*, 9138–9143; i) A. M. Shultz, O. K. Farha, J. T. Hupp, S. T. Nguyen, *Chem. Sci.* **2011**, *2*, 686–689; j) Z. Xie, C. Wang, K. E. deKrafft, W. Lin, *J. Am. Chem. Soc.* **2011**, *133*, 2056–2059; k) L. Chen, Y. Yang, Z. Guo, D. Jiang, *Adv. Mater.* **2011**, *23*, 3149–3154; l) J.-X. Jiang, C. Wang, A. Laybourn, T. Hasell, R. Clowes, Y. Z. Khimyak, J. Xiao, S. J. Higgins, D. J. Adams, A. I. Cooper, *Angew. Chem. Int. Ed.* **2011**, *123*, 1104–1107; *Angew. Chem. Int. Ed.* **2011**, *50*, 1072–1075; m) P. Zhang, Z. Weng, J. Guo, C. Wang, *Chem. Mater.* **2011**, *23*, 5243–5249; n) J.-L. Wang, C. Wang, K. E. deKrafft, W. Lin, *ACS Catal.* **2012**, *2*, 417–424; o) R. K. Totten, M. H. Weston, J. K. Park, O. K. Farha, J. T. Hupp, S. T. Nguyen, *ACS Catal.* **2013**, *3*, 1454–1459; p) Y. Xie, T.-T. Wang, X.-H. Liu, K. Zou, W.-Q. Deng, *Nature Commun.* **2013**, *4*, 1960; q) S. Yuan, J.-L. Shui, L. Grabstanowicz, C. Chen, S. Commet, B. Reprogile, T. Xu, L. Yu, D.-J. Liu, *Angew. Chem.* **2013**, *125*, 8507–8511; *Angew. Chem. Int. Ed.* **2013**, *52*, 8349–8353; r) R. K. Totten, Y. Kim, M. H. Weston, O. K. Farha, J. T. Hupp, S. T. Nguyen, *J. Am. Chem. Soc.* **2013**, *135*, 11720–11723; s) S. Fischer, J. Schmidt, P. Strauch, A. Thomas, *Angew. Chem.* **2013**, *125*, 12396–12400; *Angew. Chem. Int. Ed.* **2013**, *52*, 12174–12178; <lit t> W. Wang, A. Zheng, P. Zhao, C. Xia, F. Li, *ACS Catal.* **2014**, *4*, 321–327; u) N. Kang, J. H. Park, M. Jin, N. Park, S. M. Lee, H. J. Kim, J. M. Kim, S. U. Son, *J. Am. Chem. Soc.* **2013**, *135*, 19115–19118.
- [18] X. Du, Y. Sun, B. Tan, Q. Teng, X. Yao, C. Su, W. Wang, *Chem. Commun.* **2010**, *46*, 970–972.
- [19] For selected examples of POPs on metal-free heterogeneous catalysis, see: a) M. Rose, A. Notzon, M. Heitbaum, G. Nickerl, S. Paasch, E. Brunner, F. Glorius, S. Kaskel, *Chem. Commun.* **2011**, *47*, 4814–4816; b) Y. Zhang, Y. Zhang, Y. L. Sun, X. Du, J. Y. Shi, W. D. Wang, W. Wang, *Chem. Eur. J.* **2012**, *18*, 6328–6334; c) X.-J. Zhang, N. Bian, L.-J. Mao, Q. Chen, L. Fang, A.-D. Qi, B.-H. Han, *Macromol. Chem. Phys.* **2012**, *213*, 1575–1581; d) K. Zhang, D. Kopetzki, P. Seeberger, M. Antonietti, F. Vilela, *Angew. Chem.* **2013**, *125*, 1472–1476; *Angew. Chem. Int. Ed.* **2013**, *52*, 1432–1436; e) P. Katekomol, J. Roeser, M. Bojdys, J. Weber, A. Thomas, *Chem. Mater.* **2013**, *25*, 1542–1548; f) N. Kang, J. H. Park, K. C. Ko, J. Chun, E. Kim, H.-W. Shin, S. M. Lee, H. J. Kim, T. K. Ahn, J. Y. Lee, S. U. Son, *Angew. Chem.* **2013**, *125*, 6348–6352; *Angew. Chem. Int. Ed.* **2013**, *52*, 6228–6232.
- [20] L. Ma, M. M. Wanderley, W. Lin, *ACS Catal.* **2011**, *1*, 691–697.
- [21] a) C. Bleschke, J. Schmidt, D. S. Kundu, S. Blechert, A. Thomas, *Adv. Synth. Catal.* **2011**, *353*, 3101–3106; b) D. S. Kundu, J. Schmidt, C. Bleschke, A. Thomas, S. Blechert, *Angew. Chem.* **2012**, *124*, 5552–5555; *Angew. Chem. Int. Ed.* **2012**, *51*, 5456–5459.
- [22] C. A. Wang, Z. K. Zhang, T. Yue, Y. L. Sun, L. Wang, W. D. Wang, Y. Zhang, C. Liu, W. Wang, *Chem. Eur. J.* **2012**, *18*, 6718–6723.
- [23] a) Q. Sun, X. Meng, X. Liu, X. Zhang, Y. Yang, Q. Yang, F.-S. Xiao, *Chem. Commun.* **2012**, *48*, 10505–10507; b) E. Verde-Sesto, M. Pintado-Sierra, A. Corma, E. M. Maya, J. G. de La Campa, M. Iglesias, F. Sánchez, *Chem. Eur. J.* **2014**, *20*, 5111–5120; c) Upon the submission of this manuscript, we noticed that a TADDOL-based POP catalyst had just been reported: X. Wang, J. Zhang, Y. Liu, Y. Cui, *Bull. Chem. Soc. Jpn.* **2014**, *87*, 435–440.
- [24] a) T. E. Kristensen, K. Vestli, K. A. Fredriksen, F. K. Hansen, T. Hansen, *Org. Lett.* **2009**, *11*, 2968–2971; b) T. E. Kristensen, K. Vestli, M. G. Jakobsen, F. K. Hansen, T. Hansen, *J. Org. Chem.* **2010**, *75*, 1620–1629; c) A. C. Evans, A. Lu, C. Ondeck, D. A. Longbottom, R. K. O'Reilly, *Macromolecules* **2010**, *43*, 6374–6380; d) A. B. Powell, Y. Suzuki, M. Ueda, C. W. Bielawski, A. H. Cowley, *J. Am. Chem. Soc.* **2011**, *133*, 5218–5220.
- [25] a) M. Gruttaduria, F. Giacalone, R. Noto, *Chem. Soc. Rev.* **2008**, *37*, 1666–1688; b) T. E. Kristensen, T. Hansen, *Eur. J. Org. Chem.* **2010**, *3179*–3204.
- [26] Z. Wang, G. Chen, K. Ding, *Chem. Rev.* **2009**, *109*, 322–359.
- [27] a) R. Noyori, *Angew. Chem.* **2002**, *114*, 2108–2123; *Angew. Chem. Int. Ed.* **2002**, *41*, 2008–2022; b) W. S. Knowles, *Adv. Synth. Catal.* **2003**, *345*, 3–13.
- [28] For selected reviews on asymmetric catalysis, see: a) W. Tang, X. Zhang, *Chem. Rev.* **2003**, *103*, 3029–3070; b) P. I. Dalko, L. Moisan, *Angew. Chem.* **2004**, *116*, 5248–5286; *Angew. Chem. Int. Ed.* **2004**, *43*, 5138–5175; c) B. List, J. W. Yang, *Science* **2006**, *313*, 1584–1586; d) Y.-G. Zhou, *Acc. Chem. Res.* **2007**, *40*, 1357–1366; e) D. W. C. MacMillan, *Nature* **2008**, *455*, 304–308; f) A. Dondoni, A. Massi, *Angew. Chem.* **2008**, *120*, 4716–4739; *Angew. Chem. Int. Ed.* **2008**, *47*, 4638–4660.
- [29] a) P. Wu, C. He, J. Wang, X. Peng, X. Li, Y. An, C. Duan, *J. Am. Chem. Soc.* **2012**, *134*, 14991–14999; b) K. Mo, Y. Yang, Y. Cui, *J. Am. Chem. Soc.* **2014**, *136*, 1746–1749.
- [30] For selected reviews on heterogeneous chiral catalysts, see: a) M. Benaglia, *New J. Chem.* **2006**, *30*, 1525–1533; b) F. Cozzi, *Adv. Synth. Catal.*

- 2006, 348, 1367–1390; c) M. Heitbaum, F. Glorius, I. Escher, *Angew. Chem.* 2006, 118, 4850–4881; *Angew. Chem. Int. Ed.* 2006, 45, 4732–4762.
- [31] a) J.-L. Zhu, Y. Zhang, C. Liu, A.-M. Zheng, W. Wang, *J. Org. Chem.* 2012, 77, 9813–9825; b) G. Liu, X. Liu, Z. Cai, G. Jiao, G. Xu, W. Tang, *Angew. Chem.* 2013, 125, 4329–4332; *Angew. Chem. Int. Ed.* 2013, 52, 4235–4238.
- [32] a) D.-H. Lee, M. Choi, B.-W. Yu, R. Ryoo, A. Taher, S. Hossain, M.-J. Jin, *Adv. Synth. Catal.* 2009, 351, 2912–2920; b) L.-H. Chen, X.-Y. Li, J. C. Rooke, Y.-H. Zhang, X.-Y. Yang, Y. Tang, F.-S. Xiao, B.-L. Su, *J. Mater. Chem.* 2012, 22, 17381–17403.
- [33] D. Seebach, A. K. Beck, A. Heckel, *Angew. Chem.* 2001, 113, 96–142; *Angew. Chem. Int. Ed.* 2001, 40, 92–138.
- [34] D. Seebach, R. E. Marti, T. Hintermann, *Helv. Chim. Acta* 1996, 79, 1710–1740.
- [35] B. Schmidt, D. Seebach, *Angew. Chem.* 1991, 103, 1383–1385; *Angew. Chem. Int. Ed. Engl.* 1991, 30, 1321–1323.
- [36] P. Zhang, J. P. Morken, *J. Am. Chem. Soc.* 2009, 131, 12550–12551.
- [37] N. Momiyama, H. Yamamoto, *J. Am. Chem. Soc.* 2005, 127, 1080–1081.
- [38] a) A. N. Thadani, A. R. Stankovic, V. H. Rawal, *Proc. Natl. Acad. Sci. USA* 2004, 101, 5846–5850; b) H. Du, D. Zhao, K. Ding, *Chem. Eur. J.* 2004, 10, 5964–5970.
- [39] L. Zou, B. Wang, H. Mu, H. Zhang, Y. Song, Qu, *Org. Lett.* 2013, 15, 3106–3109.
- [40] V. B. Gondi, M. Gravel, V. H. Rawal, *Org. Lett.* 2005, 7, 5657–5660.
- [41] M. Rueping, E. Sugiono, S. A. Moreth, *Adv. Synth. Catal.* 2007, 349, 759–764.
- [42] T. Akiyama, Y. Saitoh, H. Morita, K. Fuchibe, *Adv. Synth. Catal.* 2005, 347, 1523–1526.
- [43] A. B. Charette, C. Molinaro, C. Brochu, *J. Am. Chem. Soc.* 2001, 123, 12168–12175.
- [44] S. M. Smith, J. M. Takacs, *J. Am. Chem. Soc.* 2010, 132, 1740–1741.
- [45] B. Altava, M. I. Burguete, B. Escuder, S. V. Luis, R. V. Salvador, *J. Org. Chem.* 1997, 62, 3126–3134.
- [46] S. Degni, C.-E. Wilén, R. Leino, *Org. Lett.* 2001, 3, 2551–2554.
- [47] A. Heckel, D. Seebach, *Angew. Chem.* 2000, 112, 165–167; *Angew. Chem. Int. Ed.* 2000, 39, 163–165.
- [48] B. Altava, M. I. Burguete, S. V. Luis, J. A. Mayoral, *Tetrahedron* 1994, 50, 7535–7542.
- [49] P. B. Rheiner, H. Sellner, D. Seebach, *Helv. Chim. Acta* 1997, 80, 2027–2032.
- [50] a) B. Altava, M. I. Burguete, J. M. Fraile, J. I. García, S. V. Luis, J. A. Mayoral, M. J. Vicent, *Angew. Chem.* 2000, 112, 1563–1566; *Angew. Chem. Int. Ed.* 2000, 39, 1503–1506; b) S. Degni, S. Strandman, P. Laari, M. Nuopponen, C.-E. Wile, H. Tenhu, A. Rosling, *React. Funct. Polym.* 2005, 62, 231–240.
- [51] S. Müller, M. C. Afraz, R. de Gelder, G. J. A. Ariaans, B. Kaptein, Q. B. Broxterman, A. Bruggink, *Eur. J. Org. Chem.* 2005, 1082–1096.
- [52] F. J. Uribe-Romo, J. R. Hunt, H. Furukawa, C. Klöck, M. O'Keeffe, O. M. Yaghi, *J. Am. Chem. Soc.* 2009, 131, 4570–4571.
- [53] Y.-Y. Li, X.-Q. Zhang, Z.-R. Dong, W.-Y. Shen, G. Chen, J.-X. Gao, *Org. Lett.* 2006, 8, 5565–5567.
- [54] a) M. Hatano, T. Miyamoto, K. Ishihara, *Adv. Synth. Catal.* 2005, 347, 1561–1568; b) Z. Gong, Q. Liu, P. Xue, K. Li, Z. Song, Z. Liu, Y. Jin, *Appl. Organomet. Chem.* 2012, 26, 121–129.
- [55] M.-Y. Shao, H.-M. Gau, *Organometallics* 1998, 17, 4822–4827.
- [56] L. Ma, C.-D. Wu, M. M. Wanderley, W. Lin, *Angew. Chem.* 2010, 122, 8420–8424; *Angew. Chem. Int. Ed.* 2010, 49, 8244–8248.
- [57] a) D. Seebach, D. A. Plattner, A. K. Beck, Y. M. Wang, D. Hunziker, *Helv. Chim. Acta* 1992, 75, 2171–2209; b) U. Balakrishnan, N. Ananthi, S. Velmathi, M. R. Benzigar, S. N. Talapaneni, S. S. Aldeyab, K. Ariga, A. Vinu, *Microporous Mesoporous Mater.* 2012, 155, 40–46.
- [58] L. Ford, F. Atefi, R. D. Singer, P. J. Scammells, *Eur. J. Org. Chem.* 2011, 942–950.

Received: April 8, 2014

Published online on July 25, 2014